


Project Printed Athermal Mirror

Title Executive Summary Report

Subtitle n/a
Document No. PAM-KTO-ESR-001
Issue 1.0
Date 26.08.2019


Authors

Prepared


.....
Arnd Reutlinger

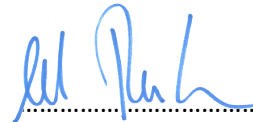
02.09.2024
.....

Technical check


.....
Sebastian Eberle

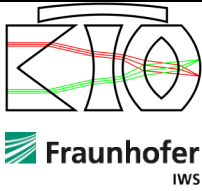
02.09.2024
.....

Approved
(Project
Manager)


.....
Arnd Reutlinger

02.09.2024
.....

This page is intentionally left blank

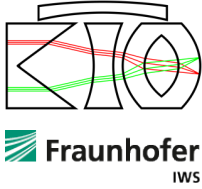


Printed Athermal Mirror

Executive Summary Report

Table of Contents

1. Abstract	5
2. Introduction	5
3. PAM Mirror Requirements	7
4. Lattice Structures	8
5. Subcomponent design	11
6. Subcomponent manufacturing	12
7. Subcomponent testing	14
8. Investigation of thermal stability (CCN)	15
8.1. Delta CTE test	15
8.2. Tempering test with disk samples	17
8.3. Change of CTE tests	19
9. Summary and Conclusion	21
9.1. Achievements	22



Printed Athermal Mirror

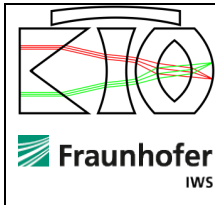
Executive Summary Report

Document Change Record

Issue	Date	DCN No. / Change description	Pages Affected
1.0	26.08.2024	Document creation	all

Document Distribution Sheet

Issue		1.0				
Issue Date		26.08.24				
Name	Company					
Christoph Wilsnack	IWS	x				
Andreas Barg	Airbus	x				
Sebastian Eberle	KTO	x				
Joel Larson	ESA	x				



Printed Athermal Mirror

Executive Summary Report

1. Abstract

Most optical instruments for space applications in the areas of earth observation, science and optical communication require high performance optical mirrors. Driving requirements are typically low Surface Form Error (SFE), high thermal stability over a wide temperature range, a low micro roughness and low mass.

A promising material combination for optical mirrors is the aluminium alloy AlSi40 as mirror substrate and electroless Nickel phosphorous (NiP) as coating for the optical surface. The main advantage of this combination is the CTE compatibility of AlSi40 and NiP over a large temperature range. In addition, NiP coated surfaces can be diamond turned and polished.

Within the ESA GSTP SME4ALM program, the feasibility to produce optical mirrors from AlSi40 by additive manufacturing (AM) was demonstrated. Main objectives were the determination of AlSi40 AM parameters and material properties as well as the demonstration of advantages of AM (e.g. topology optimization, monolithic design, lattice structures).

Based on the good results of the first project, a follow up program was launched by ESA (also in the context of ESA-GSTP) with the objective to design and print an optical mirror with TRL ≥ 5 . This executive summary summarizes the development program and results of the follow-up project, in particular:

- Identification and selection of representative mirror applications (laser communication, earth observation)
- Design and verification of optimal lattice designs for optical mirrors, inclusive cleanliness concept
- Transfer of AlSi40 printing from a lab machine to an industrial machine
- Mixed topology optimization process for mirror design
- Design, manufacturing and verification of an optical mirror with significant reduction of mass and increase of stiffness-to-mass ratio
- Thermal stability testing on sample and subcomponent level

2. Introduction

High performance optical mirrors are key components of scientific instruments in astronomy and space applications. The selection of the combination coating / mirror base material represents a primary design driver for a mirror system. Different thermal expansions will decrease the optical performance of the mirror at cryogenic temperatures. Both coating and base material must be compliant to modern high precision manufacturing (e.g. diamond turning) as well as modern polishing technologies (chemical, mechanical, ion beam).

Among the variety of materials used for mirrors, one of the most common materials is Aluminium due to its availability, thermal conductivity, low cost and ease of manufacturing. Downsides of Aluminium,

however, are its high CTE of $\sim 24 \mu\text{m}/\text{K}$ and its limited Young's modulus of $\sim 70 \text{ GPa}$. As optical space instruments in general require a very stable form, position and orientation of a few μm and arc seconds, usage of Aluminium is limited.

Therefore, in high-performance applications, where thermal and mechanical loads cannot be shielded or reduced to a level that would allow the use of Aluminium, ceramic and glass-ceramic materials such as Zerodur and SiC or other metals as Beryllium are employed.

AlSi40 material has the potential to bridge the gap between low-cost but less performant Aluminium and high performant but expensive ceramics and glass-ceramics (or even toxic materials in case of Beryllium). The CTE is reduced to about half with respect to pure Aluminium. Moreover, the mixture of Al and Si can be steered in such a way that its CTE can be matched to the one of a NiP coating, thus avoiding any bi-metallic bending effects between substrate and coating (which would be present in the case of Aluminium). The great benefit of the NiP coating is that it can be diamond turned and polished down to $\sim 1\text{nm}$ surface roughness, allowing a high performance with respect to straylight reduction.

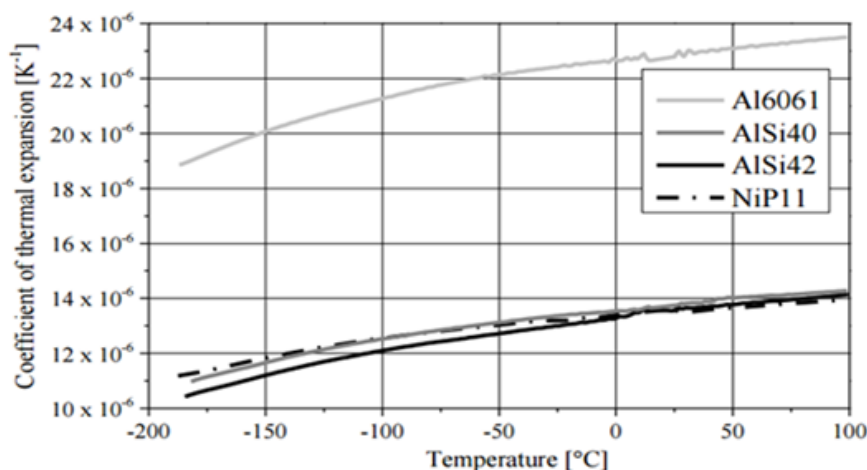
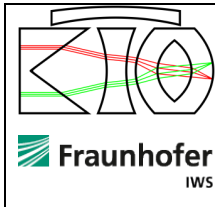


Figure 1 CTE for different aluminium alloys and NiP11 [1]

Overall, the material combination of AlSi40 for mirror body and structure and NiP coating on the optical surface allows an athermal design, i.e. a design that isotropically expands or shrinks with changing temperature but does not deviate in the optical surface form from a scaling effect in the radius of curvature. AlSi40 can thus be seen as a cost-efficient material for small and medium-sized mirrors that offers a good performance.

Additive Manufacturing (AM) offers a variety of technical features to improve the design of a structural component. It offers a high degree of design freedom which enable the manufacturing of topologically stress optimized structures, which could not be manufactured with conventional technologies, e.g. lattice structures as monolithic structures. Furthermore AM-methodologies enable the realization of complex structures from materials which usually are hard to achieve caused by the limited processability by conventional manufacturing methods (e.g. milling, forming). Utilizing Laser Powder



Printed Athermal Mirror

Executive Summary Report

Bed Fusion (LPBF) can be used for the manufacturing of complex structures composited from hollow spaces and thin structures [2].

Objective of the PAM (Printed Athermal Mirror) project was to explore the advantages of AlSi40 / NiP in combination with AM to realize high performance optical mirrors for a wide range of applications. To reach this, different expertise was joined in the team:

1. Kampf Optic Telescope (KTO): Opto-mechanical design of optical mirrors
2. Fraunhofer Institute for Material and Beam Technology (IWS): Design and development of additive manufacturing
3. Airbus Space & Defence: Large system integrator for optical instruments

3. PAM Mirror Requirements

For a mirror, the benefit of additive manufacturing is seen mainly in a reduction of mass and an increase of the stiffness-to-mass ratio beyond the means of traditional light-weighting.

Two main technical aspects were considered for the choice of an application of a PAM mirror: The optical and mechanical complexity of the mirror design and the environmental loads the mirror has to withstand.

In order to evaluate the applications, the following criteria were set by the study team:

1. Technical readiness of state-of-the art of AM and post processing of optical surface(s) and mechanical interfaces
2. Improvement of stiffness/mass ratio or “improved light-weighting”
3. Simplification of MAIT: Integral mirror & interface or several mirrors on one substrate
4. Envelope: Limited printing volume of ALM machine “Renishaw AM250/400” used in this study
5. Reduce technical risks by simple and unambiguous verification in scope of PAM project
6. Business opportunity: Reduction of costs and lead time, possible serial production of mirrors

The criteria were applied to several past and existing optical instruments (laser communication, earth observation). Two suitable applications were identified for PAM:

1. Scan- or pointing mirrors due to high stiffness to moment-to-inertia ratio
2. M1-M3 part of a TMA telescope for a compact hyperspectral application due to simplification of integration and alignment and due to the improvement of its stiffness-to-mass ratio

The small dimensions of the scanning mirror (elliptical shape with 113 x 80 mm) enabled a representative verification under thermal-vacuum cycling using a small TV chamber. Therefore, the scanning mirror was used as a subcomponent model for verification of

- Feasibility of high-performance optical surfaces
- Thermal stability of PAM over thermal-vacuum cycling

Verification of the PAM requirements on system level were planned to be performed with combined M1-M3 mirror assembly (application “2”), but not realized in the context of the project, chapter 8 “subcomponent testing”.

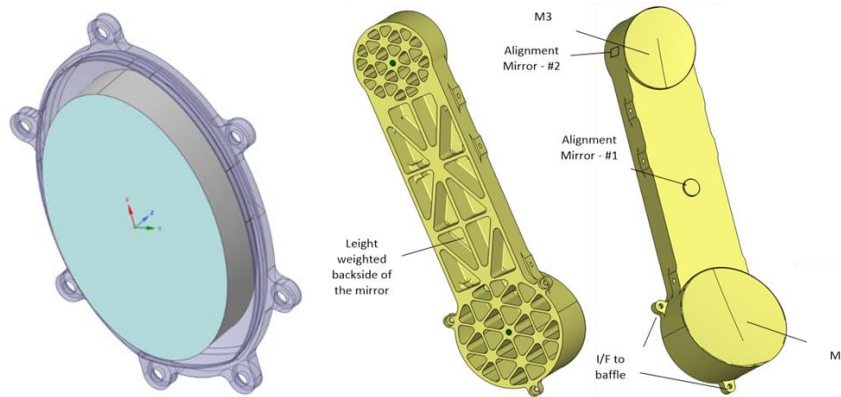


Figure 2 Selected mirror designs for PAM applications (flat scanning mirror (left) and integral M1/M3 mirror of TMA)

4. Lattice Structures

Lattice structures (internal microstructures, see Figure 3) are one of the key enablers for AM mirrors to achieve a very low aerial density. Only AM technologies can manufacture the unique geometries of lattice structures, which combine high stiffness and low mass.

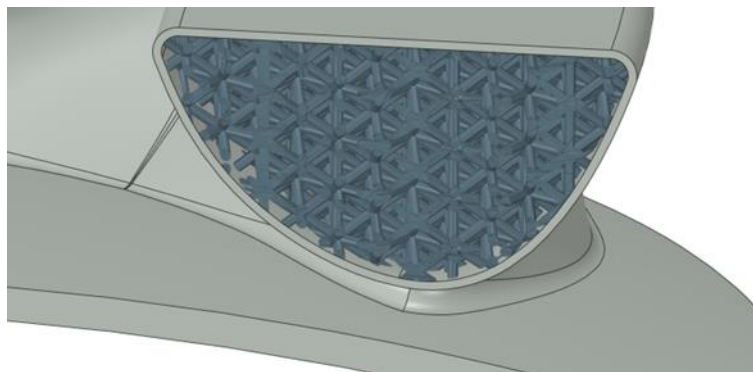


Figure 3 Cut view of AM mirror with internal microstructure, a so-called lattice structure

Based on a literature review, a set of different lattice parameters were defined:

- Lattice pattern (see following figure for potential lattice patterns, many others are possible)
- Size of single strut (min. size is determined by manufacturability by AM)
- Volume fraction (how much volume of a unit cell is occupied by printed material)

Next figure illustrates some examples for lattice structures.

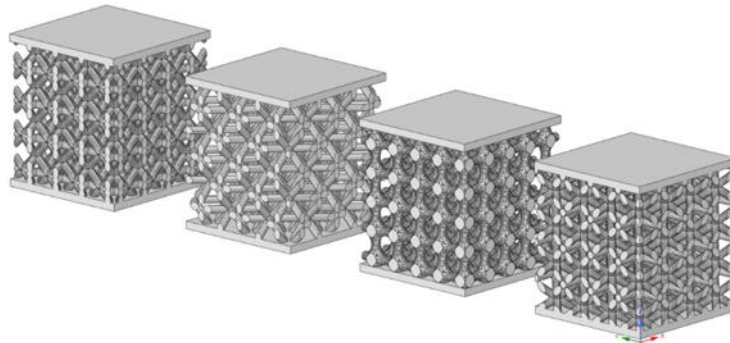


Figure 4 Examples for potential geometries of lattice structures. Test samples have a size of $20 \times 20 \times 20 \text{ mm}^3$.

A set of generic lattice structure geometries were evaluated by linear elastic finite element analysis to determine optimal lattice parameters for optical mirrors. Based on the study of lattice parameters and a parametric model of a generic optical mirrors, the following requirements were derived for lattice structures:

- The volume fraction of the lattice structures for the PAM mirror shall be between 20% to 40%, to avoid excessive form errors of the optical surface.
- The surface area of the lattice structure per volume of the unit cell coated with $50 \mu\text{m}$ of NiP shall not change the mass of the unit cell by more than 5 %.
- The elastic modulus of an internal lattice structure should be as high as possible to reduce the WFE of a generic optical mirror for space applications, particularly with respect to the diamond turning load case.
- The shear modulus should be low compared to the elastic modulus, which means that the Poisson ratio should be high.

For the lattice characterization by mechanical test, two lattice designs were selected that have a high tensile/compression modulus and a relatively low shear modulus.

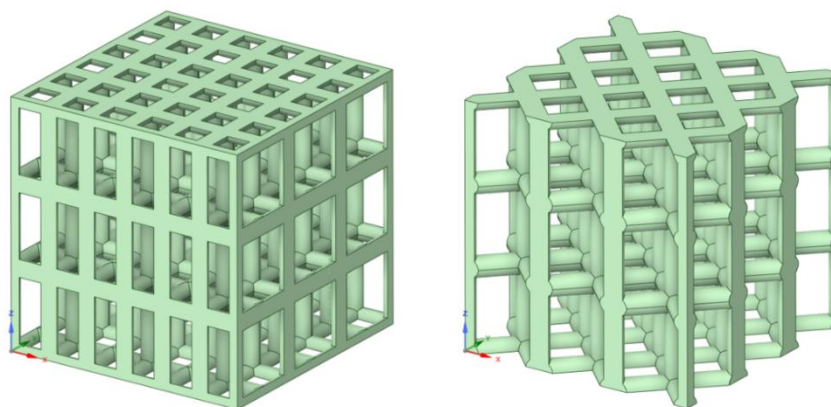


Figure 5 Two lattice designs at a volume fraction of 20%, cubic with central support (left) and “star” lattice

For manufacturing of both lattice designs the parts were rotated around 45° around the x and y axis to achieve an inclination angle of around 45° at almost every strut. For supporting cone supporting structures were applied. The part orientation on the substrate plate is illustrated in Figure 6.

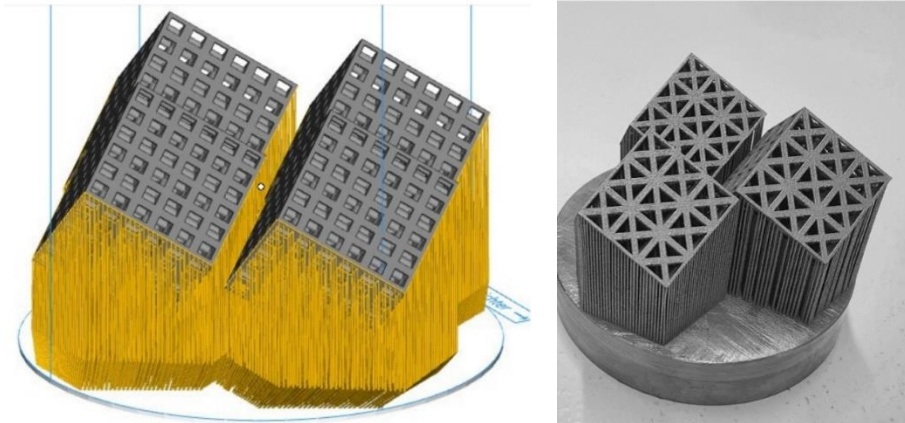


Figure 6 Supported lattice structures as design in Materialise Magics (left) and successfully manufactured lattice structures (right)

In order to characterize the impact of the optical NiP coating on the mechanical characteristics of the lattice structure, NiP coating was applied to half of the lattice sample. Compression testing of the lattice cubes was carried out on a MTS 810 compression testing machine.

The graphical representation in Figure 7 shows a significant improvement of the respective compression strengths of each lattice type by almost 200 % after NiP coating. Apparently, the NiP coating dramatically enhanced the stiffness of the lattice structures. Moreover, the coating might have covered some of the surface irregularities (roughness, attached particles, ...) which otherwise might have acted as crack-initiating defects.

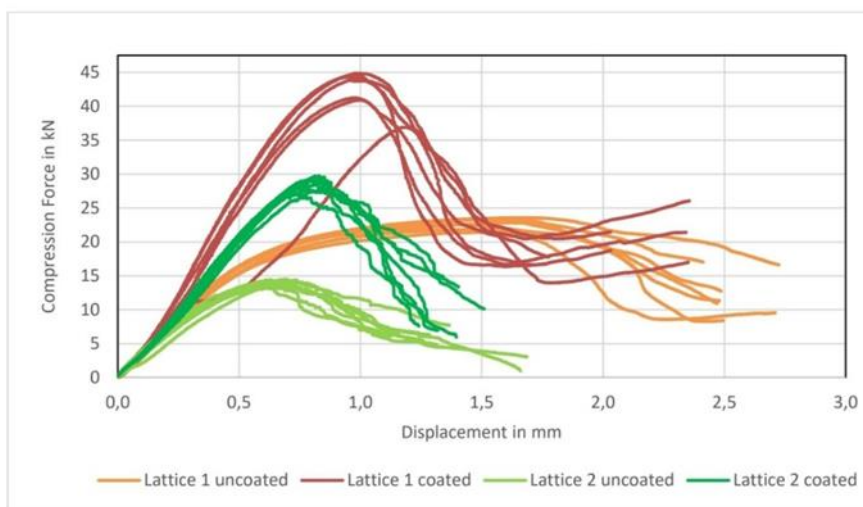


Figure 7 Compression force - displacement curves for tested lattice samples

Table 1 Results of the compression testing

	ΔL at $F_{Comp.max}$ in mm	Global Elongation at $F_{Comp.max}$ in %	Strength in N/mm ²	Elastic Stiffness ¹ in kN/mm
Lattice 1 – uncoated	1.52	5.08	126.31	36.16
Lattice 1 – coated	1.01	3.35	235.38	57.23
Lattice 2 – uncoated	0.65	2.17	77.50	29.50
Lattice 2 – coated	0.80	2.67	158.37	44.12

5. Subcomponent design

The PAM subcomponent design is based on a scanning mirror for laser communication. The elliptical mirror with the dimension of 113 mm (long axis) and 80 mm (short axis) has to be compliant to:

Operational temperature range: -30° - +80°C

- Mass: < 200 g
- First natural Eigenfrequency: > 800 Hz
- Surface Form Error: < 12 nm rms
- Surface roughness: < 1 nm Ra

In addition to high vibration and shock loads, a pressure load of 7.5 kN for Diamond Turning (DT) was considered in the design. The mirror envelope and some parameter variations of it were assessed to understand the driving design parameters and the potential for AM specific design.

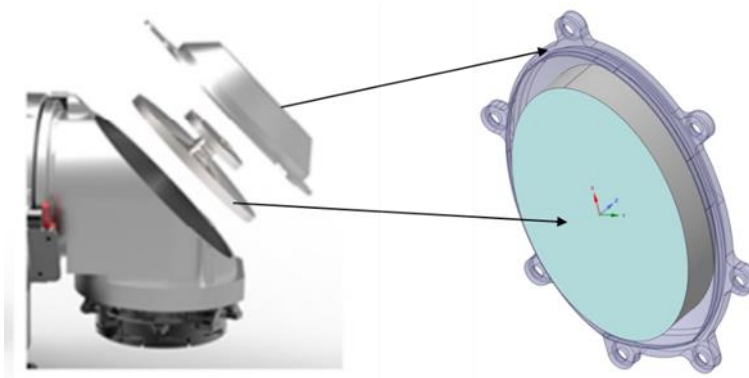


Figure 8 Explosion view of laser scan mirror (left), envelope of mirror with cap

The mass requirement can only be reached by light weighting design. In order to compare the AM topology optimized design, a sandwich structure design was used for comparison. Main goal for the topology optimization was selected for maximum strength to increase the mirror performance wrt SFE.

The two developed designs were verified for the same load cases as the baseline design to determine mass, first eigenfrequency and the WFE at ambient temperature and at operational conditions. A NiP coating of 50µm was assumed on the optical surface. Next table summarizes the results of the conventional sandwich and the AM optimized topology design.

Table 2 Results of assessment of two mirror designs

Internal design	Requirement	Honeycomb	Mixed topology (Lattice 20%)
Mirror mass, g	<200	163	200
1. Eigenfrequency, Hz	>800	1232	1300
WFE at ambient, nm	<10.7	5,9	2,8
WFE at operation, nm	<14	8,8	6,1

Although the mirror with traditional light-weighting is lighter, the AM specific design achieves a higher eigenfrequency and lower WFE at ambient and at operation. Next figure illustrates the mixed topology design.

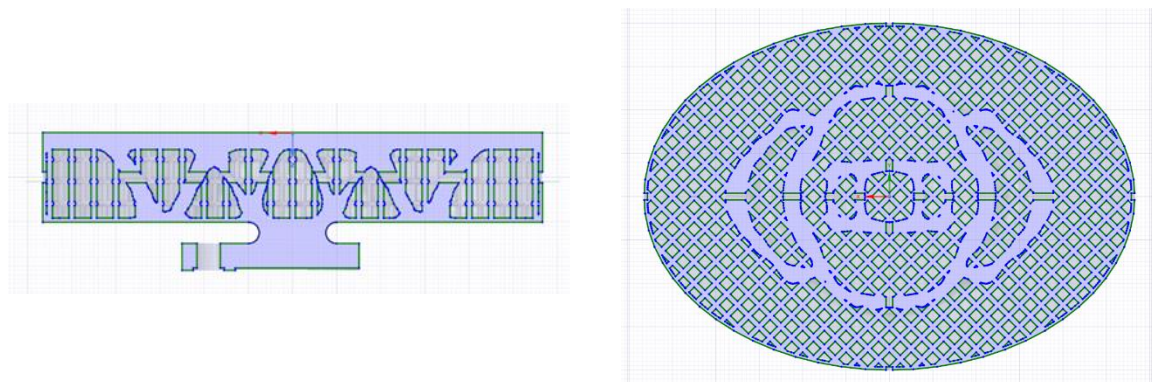


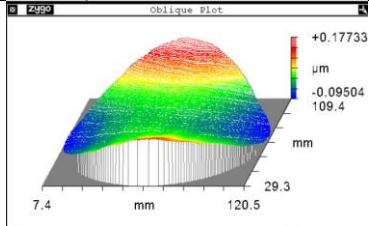




Figure 9 Cut through mixed topology design with internal voids filled with star lattice at 20% volume fraction.

6. Subcomponent manufacturing

The subcomponent manufacturing encompasses the following manufacturing steps:

<p>1. Printing in 45° angle with (optical surface upside)</p>	
---	--

2. Post-machining of mechanical interface and mirror backside	
3. First DT of optical surface	
4. Application of NiP coating ~75 μm	
5. Second DT of optical surface	
6. Polishing	

In order to reach the optical surface specification, the subcomponent was also polished by the Technische Hochschule Deggendorf. By application of a stepwise approach using classical polishing and Magneto Rheological Finishing (MRF). Next table summarizes the mirror properties after DT and polishing.

Table 3 Properties of optical surfaces after diamond turning and polishing

Requirements	Diamond Turning	Polishing
WFE rms < 12 nm	n/a	9,3
WFE PV < 97 nm	272	89,3
Roughness < 1 nm Ra	2,64	1,5

The requirement of surface roughness is slightly not compliant. It turned out that the used polishing technologies enabled either full compliance of SFE or surface roughness. The delta from 1,5 nm Ra to the required 1.0 nm Ra was considered negligible.

7. Subcomponent testing

The subcomponent was tested with thermal vacuum cycling in following temperature ranges:

- Operating temperature range from -30°C to $+80^{\circ}\text{C}$
- Non-operational temperature range from -30°C to $+105^{\circ}\text{C}$

The subcomponent was mounted on a cooling/heating plate inside a thermal vacuum chamber (TVC). To measure the wavefront error (WFE) of the optical surface of the subcomponent, an optical set-up was placed outside the TVC. The measurements were performed in double-path configuration through an optical window in the TVC.

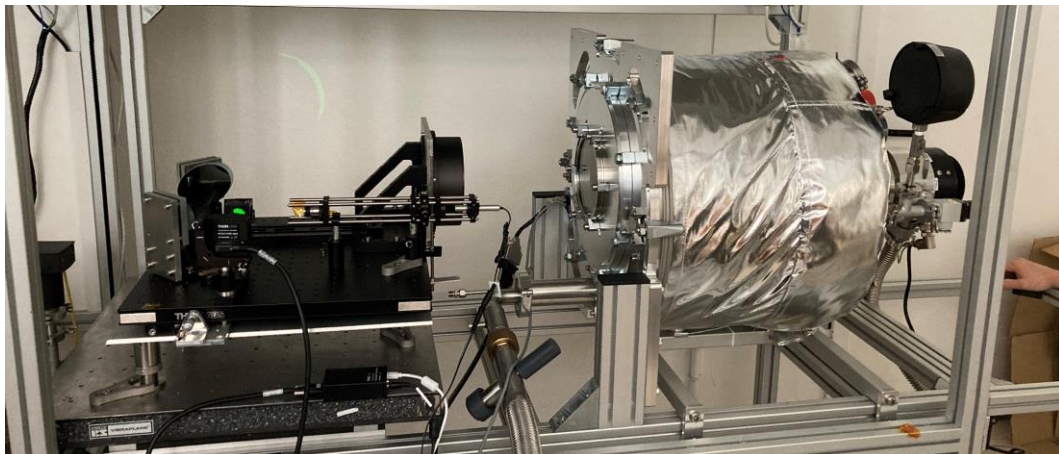


Figure 10 Test setup of PAM thermal vacuum tests

Twelve thermal cycles were performed to determine PAM thermal stability. The WFE of the subcomponent increased substantially over the course of the twelve TV cycles measured at RT and particularly at -30°C operational temperature.

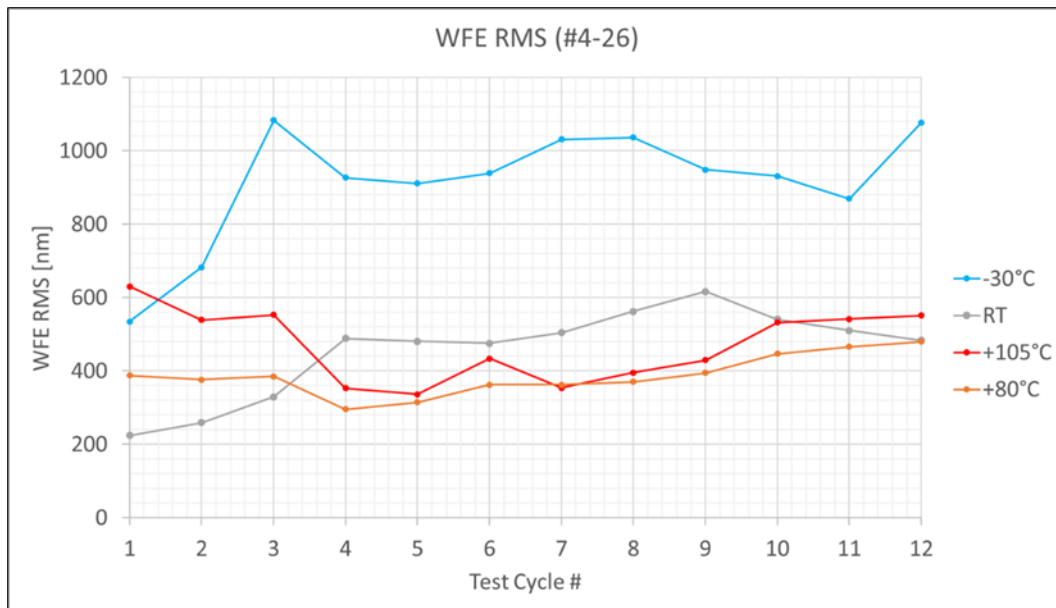


Figure 11 WFE of SUB in vacuum at each temperature over twelve test cycles.

The thermal stability of the subcomponent was several orders of magnitude out of spec. The project partners therefore decided to issue a CCN for the stepwise investigation and improvement of the thermal stability of AM AISi40 on sample, sub- and component level.

8. Investigation of thermal stability (CCN)

The thermal stability investigation was divided into:

- CTE mismatch between AM AISi40 and NiP plating using beam samples
- Tempering tests by applying thermal cycling on flat mirror disc samples after NiP plating and before final machining by diamond turning
- Change of CTE in dependence on the sample orientation wrt AM printing

8.1. Delta CTE test

NiP coatings with 100 and 200 μm thickness was applied only to one side of the beam sample to enable a bi-metallic effect. CTE was calculated based on the beam deflection in a thermal chamber during thermal cycling.

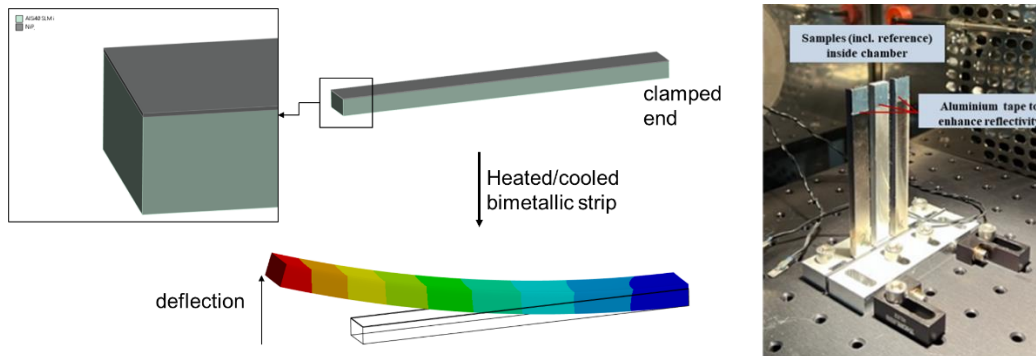


Figure 12 Beam sample, bi-metallic effect (left), installed in the thermal chamber

The response of the six tested beam samples was in-homogeneous to temperature changes. To better understand the responses of the tested samples an analytical model, inclusive variations of the main parameters (beam thickness, NiP plating thickness) was fitted to the test results with the delta CTE between AlSi40 and NiP as the driving parameter.

The difference in CTE between NiP and AlSi40 observed in this experiment amounted to 1.1 ppm/K at -28°C and 0.5 ppm/K at $+80^{\circ}\text{C}$, which is larger than the results from previous CTE measurements on these materials.

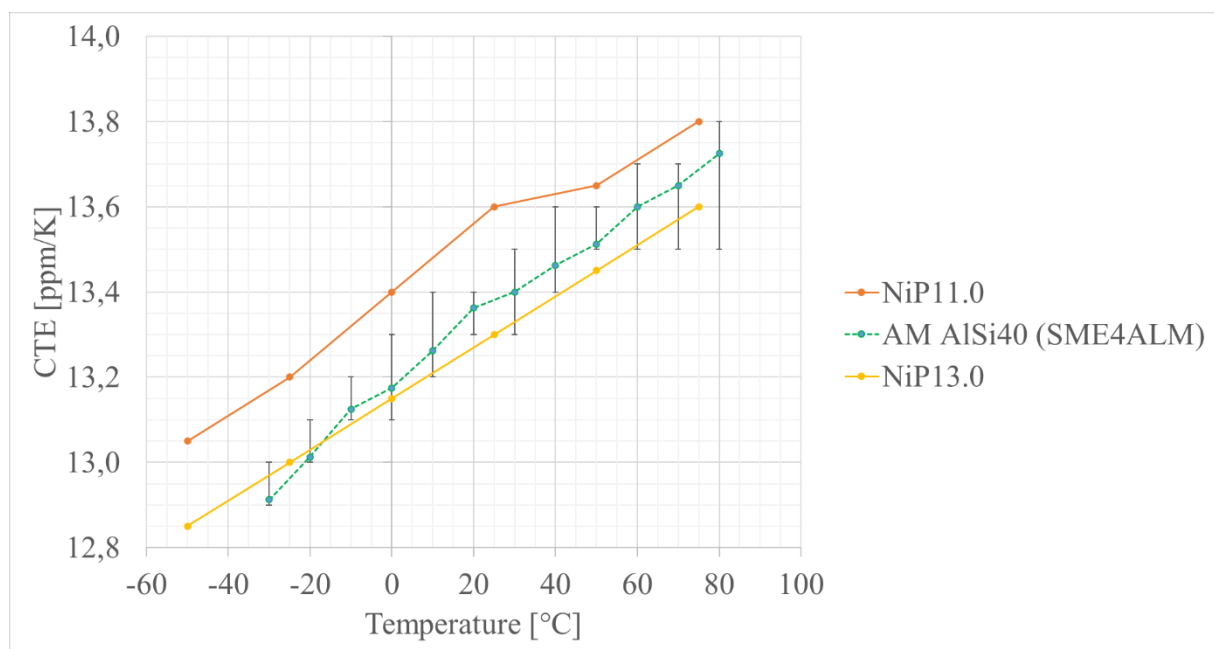


Figure 13 CTE of AM AlSi40 from precursor project compared to CTE of NiP with different P-content

The observed delta CTE was acceptable and not found to be the driver for the large mirror surface deformations seen in the subcomponent TV tests.

8.2. Tempering test with disk samples

Four disc samples of 100 mm diameter and 20 mm thickness were additively manufactured with AlSi40 of the same powder batch as the previous models and samples. Two of the four disc samples were tempered after AM, NiP plated, and thermally cycled before final machining by diamond turning to achieve a flat mirror surface. The thermal cycling before the final machining was performed to improve thermal stability of the optical surface, based on the results of the subcomponent TV tests.

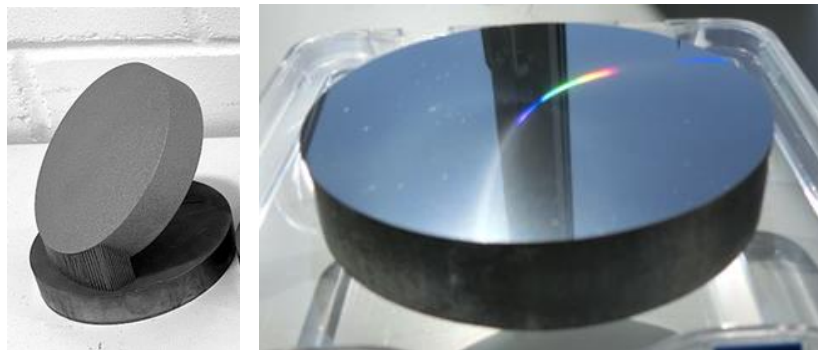


Figure 14 Disc sample after AM (left), finished mirror after diamond turning

To verify the thermal stability of the disc samples, their SFE was measured at RT before the test campaign and then between thermal cycles. The disc samples were put in a thermal chamber for thermal cycling. To protect the mirror surface against dirt and condensation in the thermal chamber, the discs were put in a sealed container and purged with dry nitrogen before every thermal cycle.

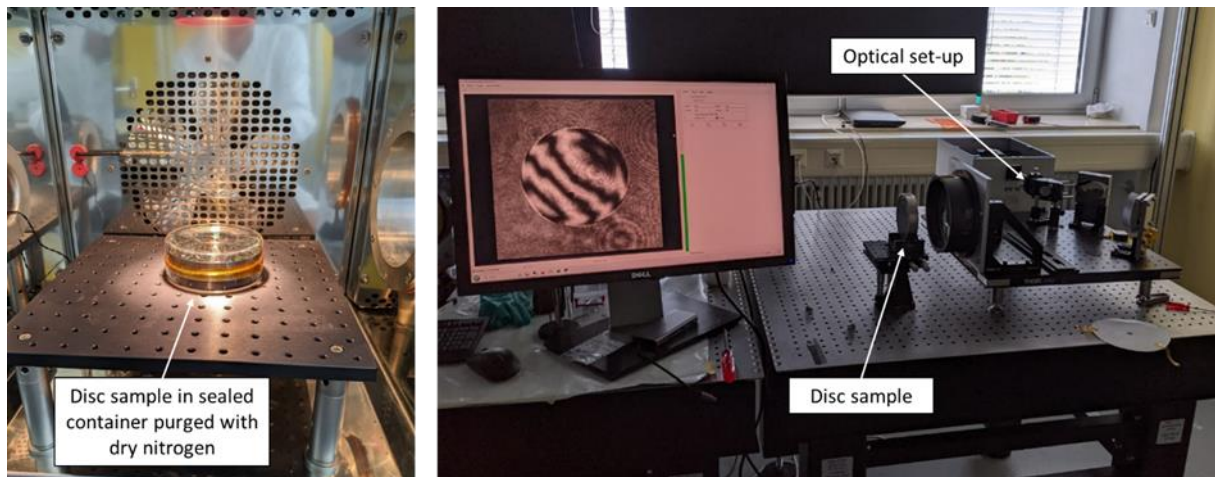


Figure 15 (left) Disc sample in thermal chamber. (right) Optical set-up to measure SFE of disc samples.

Disc sample #01 underwent 49 thermal cycles and disc sample #02 underwent 40 thermal cycles. Optical measurements were not taken after every thermal cycle. Despite the thermal treatment of the discs during manufacturing, the SFE of the flat mirror samples increased almost linearly over the number of thermal cycles (see figure 16).

Based on experiments on the thermal stability of bulk AlSi4x mirrors, it was expected that thermal stability of the two disc samples is reached after about 5-10 cycles. Since thermal stability was not reached even after 40 to 49 cycles, it was decided to end the experiment.

To verify, if the hot or the cold temperature inflicted the residual deformation in the disc samples, both samples were held at +105°C for 48h before a further optical measurement at RT and then held at -30°C before a further optical measurement at RT. Surprisingly, these extra thermal treatments had almost no effect on the SFE of the mirror samples (see following two figures).

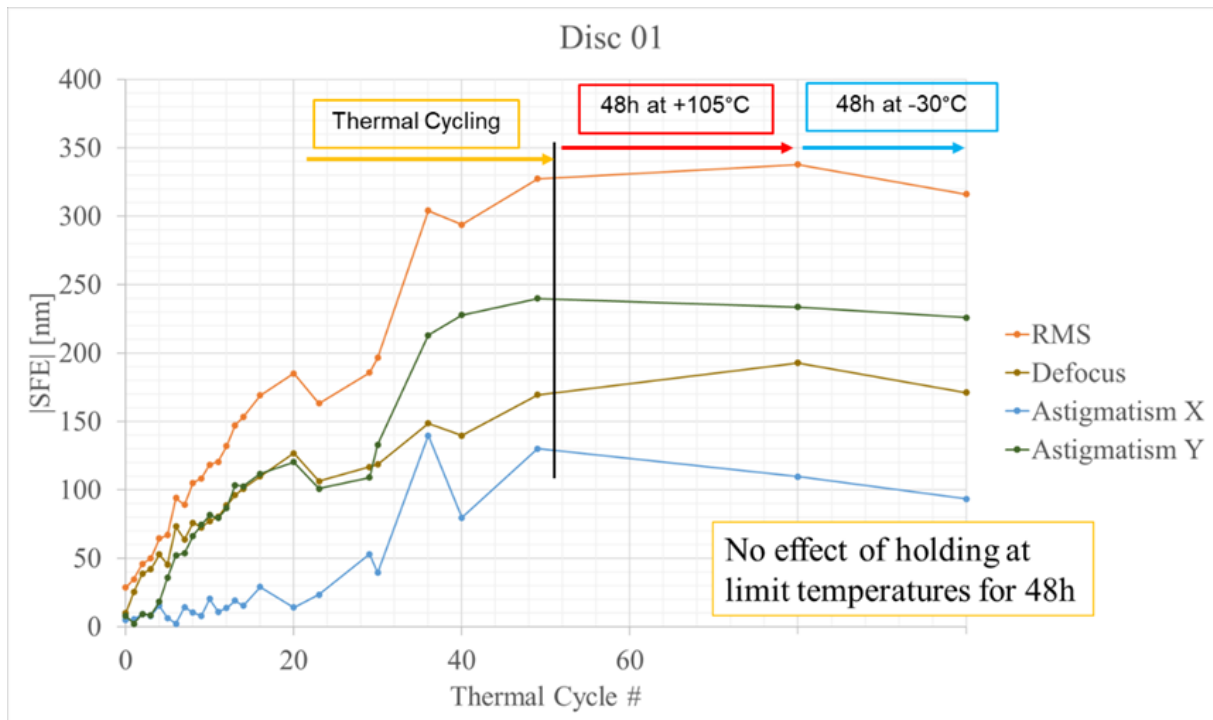


Figure 16 SFE in terms of RMS and main Zernike coefficients of disc sample 01 over 49 thermal cycles and additional holding at limit temperatures.

To better understand the residual deformation of the mirror surfaces due to thermal cycling, the SFE was decomposed by Zernike polynomials. The main contributors to the SFE were defocus and astigmatism.

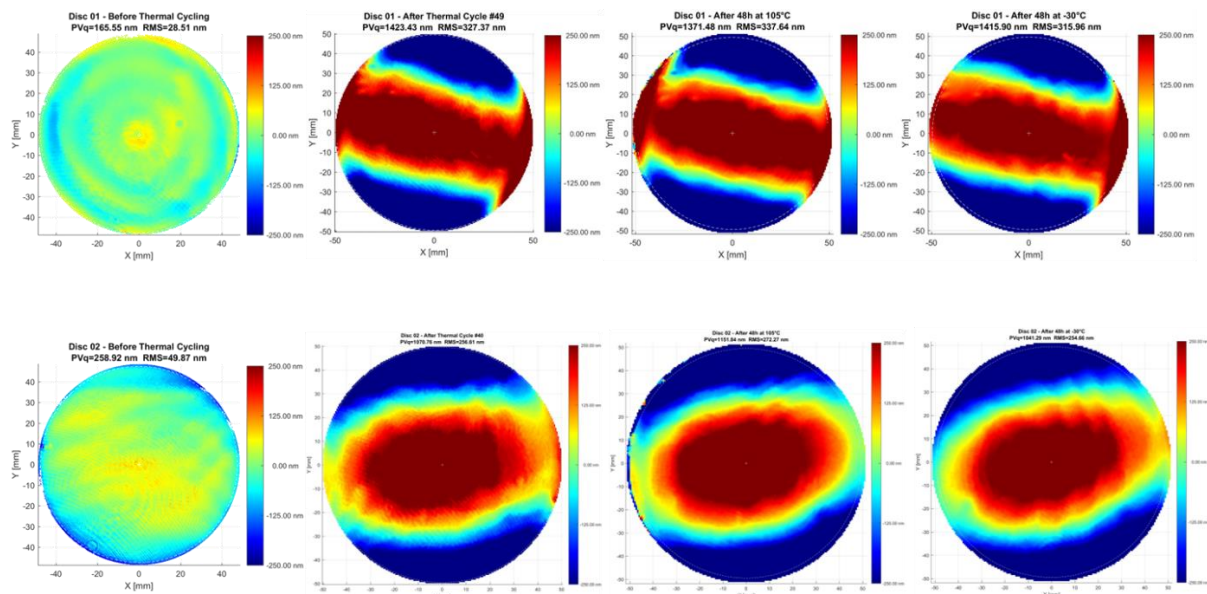


Figure 17 Evolution of SFE in terms of RMS of disc samples over thermal cycles and additional holding at limit temperatures.

The following conclusions were drawn from the thermal cycling experiment on two disc sample mirrors:

- AM AlSi40 mirrors with NiP plating are not thermally stable, even when they are tempered and thermally cycled before final machining of the optical surface.
- This result is in contradiction to the experimental findings on bulk AlSi4x mirrors
- The increasing astigmatism over thermal cycles pointed to an orthotropic state of stress in the mirror samples, which might be related to the layer-wise manufacturing by SLM.
- It was hypothesized that the CTE of AM AlSi40 changes differently over thermal cycles depending on the orientation to the printed layers.

To investigate this hypothesis, it was decided to cut CTE samples out of the remaining two discs for dilatometer measurements, which were not NiP plated. The budget of the work package “Transfer to subcomponent level” was used for these measurements.

8.3. Change of CTE tests

To verify, if the CTE of AM AlSi40 changes differently per orientation to the printing process due to thermal cycling, CTE tests were performed with a Dilatometer.

Three cylindrical test samples of 6 mm diameter and 15 mm length were cut out of one of the two disc samples that were kept as spare (see ch. 4.3.1). The three samples were cut out of the disc in three different orientations (see figure 18). Each cylindrical test sample represented one of the three main directions of the additively manufactured discs.

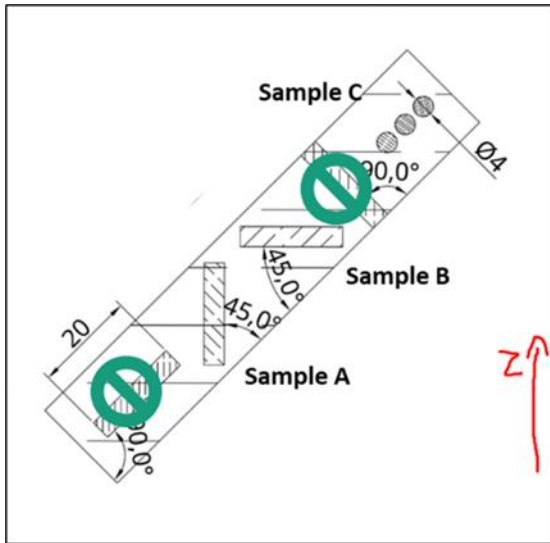


Figure 18 (left) Orientation of CTE samples relative to build-up direction of additively manufactured disc (red arrow). (right) Dilatometer used for CTE tests.

The CTE test samples underwent nine test cycles btw. -50°C and $+105^{\circ}\text{C}$ with a holding time of 20 min at the limit temperature levels.

The results of the three samples already showed that the CTE of sample C (in-plane) stayed within a very small range and did not really change. Compared to that, the CTE of sample A (out-of-plane) changed significantly. This is even more evident, when the CTE of the first measurement is subtracted from the last measurement (see figure below).

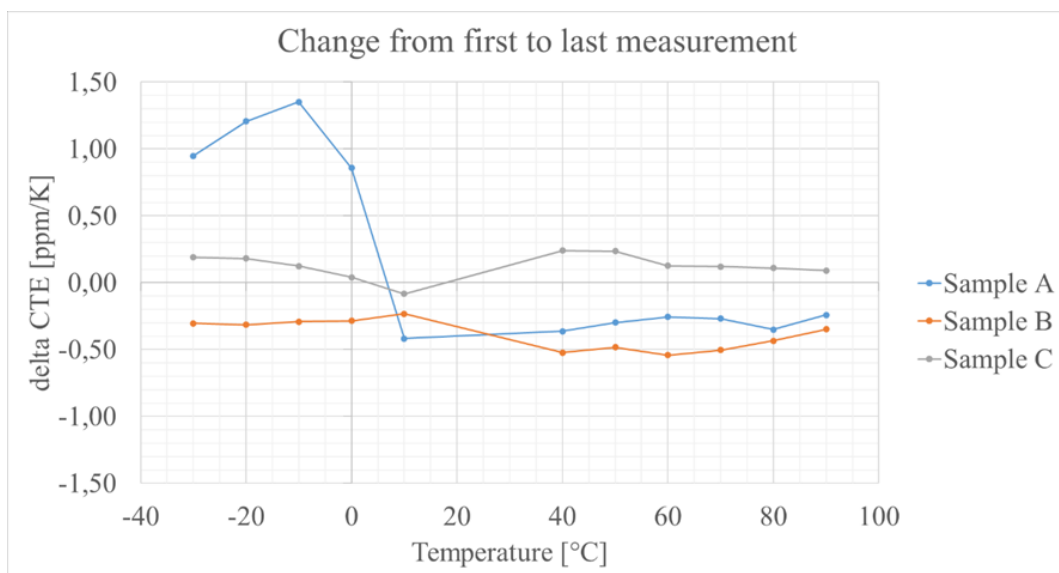


Figure 19 Change of CTE from first to last measurement for each sample

To understand the effect of the observed change in CTE per “printing” direction of the AM process on the deformation of the disc mirror samples, a FEA was performed with the experimentally determined CTE data. With the orthotropic and temperature depend CTE data and a NiP plating of 75 μ m on the mirror surface and 100 μ m on the rest of the mirror, a thermo-elastic analysis was performed at +100°C and -30°C. The deformations of the mirror resulted in the following SFE (Zernike #1 to #3 removed).

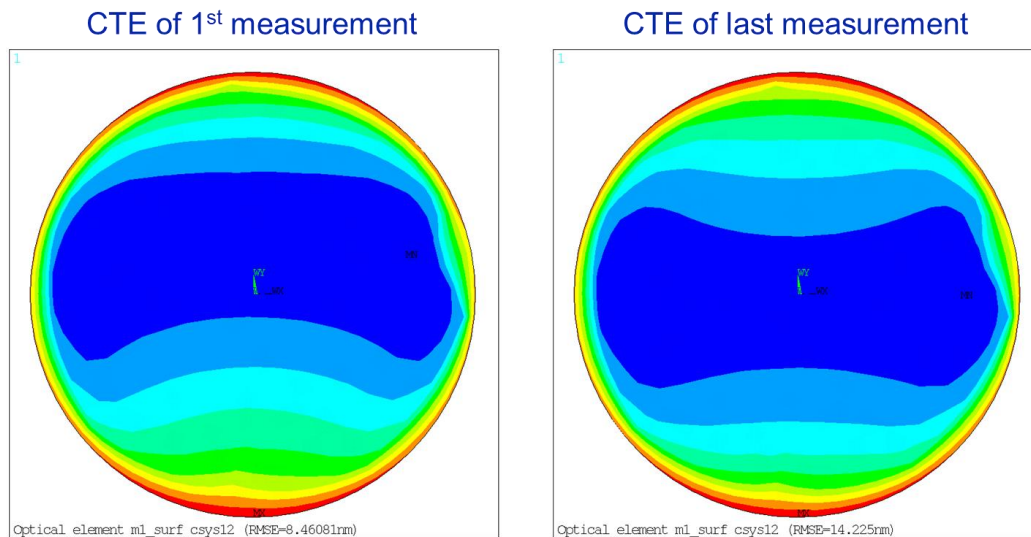


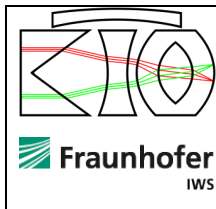
Figure 20 Computed SFE of disc sample with orthotropic CTE data from tests at +100°C.

The following conclusions were drawn from the CTE tests:

- The CTE of AM AlSi40 changed more in out-of-plane direction than in in-plane direction due to thermal cycling
- The out-of-plane CTE changed differently in the positive and the negative temperature range.
- The determined orthotropic CTE resulted in astigmatism of a flat mirror FE-model with the configuration of the tested disc samples (see ch. 4.3.3).
- The change of CTE due to thermal cycling increased the SFE of the flat mirror FE-model by +68% at +100°C and +57% at -30°C.
- A different orientation of astigmatism developed in the flat mirror FE-model for +100°C and -30°C.

9. Summary and Conclusion

The main objective of the project “Printed Athermal Mirror” (PAM) was to bridge the gap between TRL4 and TRL5 for an additively manufactured mirror made of AlSi40 with NiP plating and to demonstrate the potentials of additive manufacturing for space missions and products.



Printed Athermal Mirror

Executive Summary Report

This objective was not achieved. A fully space qualified mirror made of AM AlSi40 with NiP plating could not be developed. The main obstacle in applying this technology to a space mirror was the lack of thermal stability in terms of optical performance, which was verified on different levels of complexity:

- Thermal vacuum tests of a subcomponent (flat mirror for laser communication) resulted in an increased WFE over twelve thermal cycles without reaching stability
- To improve the thermal stability of the used material mix, thermal cycling within the non-operational temperature range of the subcomponent was applied to flat disc mirror samples before final manufacturing of the optical surface. However, the thermal stability of the flat disc mirror samples was not improved by the thermal treatments during manufacturing (see ch. 4.3.3 for details). A progressively increasing astigmatism of the flat mirror samples over thermal cycles pointed to an orthotropic state of stress in the mirror samples, which might be related to the layer-wise manufacturing by SLM. It was hypothesized that the CTE of AM AlSi40 changes differently over thermal cycles depending on the orientation to the printed layers.
- To investigate, if the CTE of AM AlSi40 changes differently per orientation to the printing process due to thermal cycling, CTE tests were performed on one AM AlSi40 sample per main orientation to the printed layers (see ch. 4.3.4 for details). The tests revealed that the CTE of AM AlSi40 changed more in the out-of-plane direction than in the in-plane direction due to thermal cycling. In addition, the out-of-plane CTE changed differently in the positive and the negative temperature range.

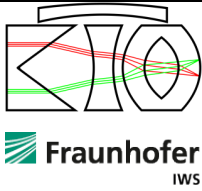
The main conclusion of the PAM project is therefore, that with the currently available material and AM process parameter a printed AlSi40 mirror with NiP coating is not thermally stable, even when the mirrors are tempered and thermally cycled before final manufacturing of the optical surface.

It is rather unclear whether the observed thermal instability of the printed AlSi optical mirrors is due to the 3D-printed nature of the PAMs or whether it originates from the AlSi40 material itself. A direct comparison between the two is needed by manufacturing the same disc samples with traditional manufacturing and additive manufacturing methods and testing the two under identical conditions. If a better performance is observed for bulk AlSi, we should perform a microscopic analysis of the printed material to further study the effects of gaps, dislocations, relaxations and internal stresses in the printed internal structure. The internal structure for light-weighting should also be carefully considered as a potential cause for thermal instability.

9.1. Achievements

Despite the missed main objective of the project, several technological improvements were achieved:

- With the flat mirror for laser communication, a space product was identified that could benefit from the combination of additively manufactured AlSi40 and NiP plating due to improved lightweighting, an improved optical performance, and a very low micro-roughness and WFE of the optical surface (see ch. 4.1.8 for details).
- It was found that additively manufactured microstructures benefit immensely from a NiP plating. A NiP coating not only improved the cleanliness of lattice structures by binding any powder



Printed Athermal Mirror

Executive Summary Report

particles left after manufacturing, it also increased the stiffness of the tested lattice structures by at least 50% and their strength by at least 86% (see ch. 4.1.2 for details).

- A mixed topology optimization approach was developed that allowed the design of lightweight and high-performance mirrors. A special focus was put on the inclusion of manufacturing loads and constraints for the design of mirrors that maximize the benefits of additive manufacturing (see ch. 4.1.5).
- An AM specific design of the FORUM telescope M1-M3 mirror was developed that is almost 20% lighter than a conventionally manufactured design with an almost 50% higher eigenfrequency, while having the same or better optical performance (see ch. 4.2.3).